JOURNAL OF MATERIALS SCIENCE 22 (1987) 193–201

Surface crystallization behaviour of Metglas 2605-SC and 2826-MB

A. SCHERER, O. T. INAL*
Department of Metallurgical and Materials Engineering, New Mexico Institute of Mining and Technology, Socorro, New Mexico 87801, USA

The crystallization behaviour of two quaternary amorphous alloys, Metglas 2605-SC and Metglas 2826-MB, were investigated by reflection electron diffraction observations of *in situ* heat treatment. The surface crystallization phenomena of these materials were compared to those of the bulk, in particular with respect to the structures of the initial metastable crystallization products. Anisotropic crystallization of the surfaces was observed on both of these ribbons, indicated by oriented arc patterns of the initial crystallites. This effect was determined to be a result of local elemental depletion of the surface layers.

1. Introduction

During the heat treatment of amorphous metal ribbons, differences between the surface and bulk crystallization are commonly observed. In some amorphous metals, such as Metglas 2826-MB†, crystallization is observed to propagate from the surface into the bulk of the ribbon [1], whereas in other Metglasses, such as 2605-SC†, the initial surface crystallization products are found to differ from those of the bulk [2]. This has in the past been explained by differences in the chemical constituency of the ribbon surfaces [3], or the existence of surface oxide films which can provide heterogeneous nucleation sites. Since an understanding of the crystallization phenomena in commercial amorphous alloys is very important in determining their thermal stability, structural and chemical differences between the crystallization products at the surface and inside the ribbon have to be explained.

Techniques generally used for the analysis of amorphous metals include transmission electron microscopy (TEM) [4], field ion microscopy (FIM) [5], X-ray diffraction (XRD) [6], neutron diffraction [1], Mossbauer spectroscopy, differential scanning calorimetry (DSC) [7], small-angle X-ray scattering (SAXS) [8], and resistometer experiments [2]. Preparation of samples for the initial two techniques requires electropolishing or etching away of the surface layers, whereas the latter techniques generally sample more than 2000 nm into the ribbon. Surface analysis techniques such as Auger electron spectroscopy (AES) [9, 10], energy dispersive X-ray analysis (EDS), and conversion electron Mossbauer spectroscopy (CEMS) [3, 11] have only recently been performed to observe the surface crystallization phenomena in amorphous ribbons. These techniques provide information on the composition of the surface as well as the atomic bonding and short-range order during thermal exposure of the ribbons. However, structural information on a larger scale is not available from these techniques, and *in situ* observation of the ribbon surfaces during crystallization is not easily accomplished.

A technique developed in the early 1930s, reflection electron diffraction (RED) [12], is ideally suited for the *in situ* analysis of surface crystallization phenomena in amorphous alloys. Using this technique, the influence of the heating rate and exposure temperature on the crystallization products of Metglas 2605-SC and 2826-MB are investigated, and the differences in the structures of crystallization products on either side of the ribbon are compared. These experiments are performed to identify and describe the factors which determine the surface crystallization of amorphous metglas ribbons.

2. Procedure

2.1. Sample preparation

Ribbons of Metglas 2826-MB and 2605-SC, manufactured by Allied Chemical Corporation, were found by previous RED analysis [12] to contain localized areas of surface crystallites, which were identified as copper and its oxides. The surface layer of the ribbons could be removed by an anodic etch in 5 vol % sulphuric acid at 1.5 A dm^{-2} for 2 min, followed by a cathodic etch in a separate bath under the same conditions, which also dissolved these crystallites. Such preparatory treatment, however, invariably forms a thin oxide film on the ribbon surface, and dry mechanical grinding of samples was found to be the most effective way to provide clean amorphous metal.

2.2. RED, XRD and SEM

An RCA EMU-3G TEM was equipped with a reflection electron diffraction stage and operated at 100 kV, in transmission reflection electron diffraction mode [12]. The metglas ribbons were bent and oriented near-parallel to the electron beam to improve the diffraction

*Author to whom all correspondence should be addressed.
†Tradename, Allied Chemical Corporation.

0022–2461/87 $03.00 + .12

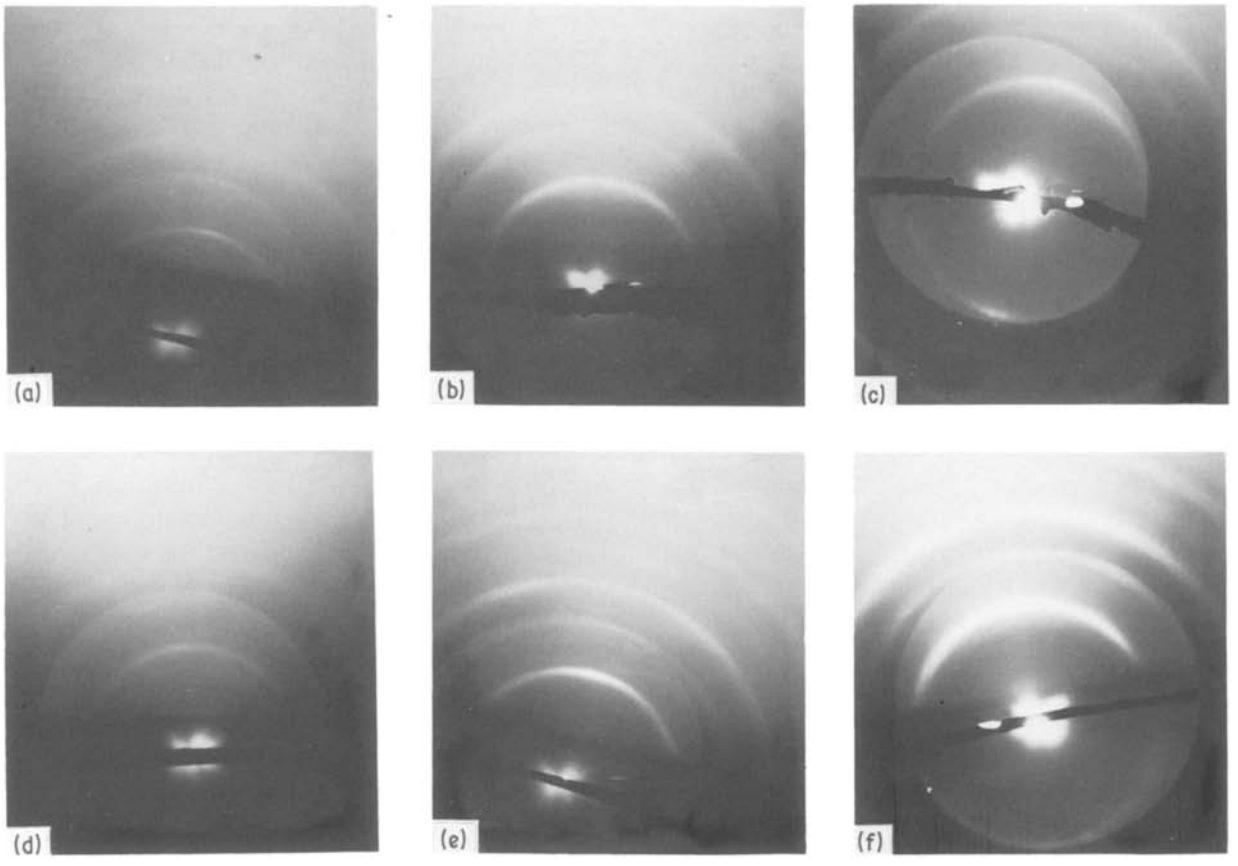

Figure 1 (a, b) RED sequence taken during the crystallization of the bright side of Metglas 2605-SC with a heater current of 1.3 A; (c) RED pattern showing both bright and dull side of the ribbon; (d–f) RED sequence taken with a heater current of 1.7 A.

pattern brightness. Since RED patterns are not only dependent on the composition and the structure, but also the surface morphology, SEM micrographs were obtained before and after heat treatment, in a Hitachi HHS-2R SEM, to describe the surface morphology. Heat-treated samples were also analysed by XRD to obtain information on the near-bulk crystallization products and to provide a comparison with reflection electron diffraction patterns.

2.3. Heat treatments

In situ heat treatments were performed using a resistive heater located behind the specimen. The heater temperature was monitored with a thermocouple, and time–temperature curves were recorded for all *in situ* experiments. In this arrangement, the measured heater temperature could be increased from room temperature to 773 K within 5 min. The thermocouple was placed next to the specimen in this study to provide relative time–temperature data during heat treatments. Although the heat treatments were found to be very reproducible, the absolute measurement accuracy was approximately $\pm$ 20° C.

2.4. Deposition techniques

Oxidation of specimens for this study was achieved by immersion in distilled water, followed by air-drying. Au–Pd sputtering was performed in a sputter deposition unit, and coatings of approximately 10 nm were deposited, as determined from standard calibration curves. Electrodeposition of platinum was done in a chloroplatinic acid solution with 1 g l^{-1} $PtCl_4 \cdot H_2O$ with a galvanostat at 10 mA. The resulting deposits varied from 1.2 to 120 nm in approximate thickness estimated by the use of Faraday's law.

3. Results and discussion

3.1 Metglas 2605-SC

3.1.1. Heat treatments

Previous studies analysing the crystallization behaviour of 2605-SC have determined the first crystallization product in the bulk to be α-ferrite [13]. At higher temperatures (> 823 K), this product combines with Fe_3B and $Fe_{23}(C, B)_6$ [2] to be formed in the partially crystallized ribbons. It was, however, found to be very difficult to avoid surface oxidation during heating in Argon-purged furnaces, and the crystallization products of the ribbons could not be observed with RED without prior surface cleaning. During such cleaning, the immediate surface layer is generally removed, and only the bulk crystallization behaviour of the ribbon is observed. To avoid this problem, *in situ* heating in the reflection electron diffraction chamber was performed.

If the free (and shiny) surface of 2605-SC is observed during a heat-treatment experiment in the RED chamber, the resulting diffraction pattern consists of smooth rings corresponding to ferrite (Figs 1a, b, d to f). This pattern remains apparently unaffected by changes in the heating rate [14]. The temperature curves recorded during these heat treatments are summarized in Fig. 2. Fig. 1c shows a RED pattern which combines information from both sides of the ribbon simultaneously, and ferrite is found to be the

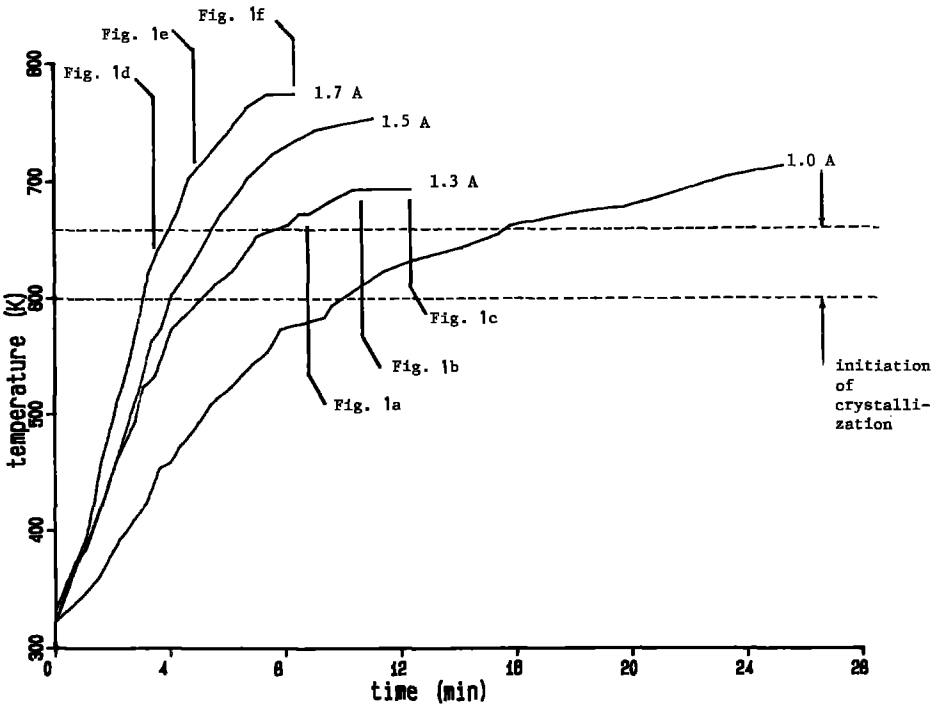

Figure 2 Time–temperature curves for heat treatments of the bright side of Metglas 2605-SC measured during *in situ* heat treatment.

predominant product at both surfaces during crystallization. However, the ferrite pattern on the wheel (rough) side of the ribbon is found to consist of ferrite arcs, which indicates that the crystallites on the surface follow a distinct surface orientation. This surface orientation can be matched to the [1 1 1] orientation (Fig. 3), indicating that the [1 1 1] direction in the crystallites is oriented perpendicular to the ribbon surface. This effect can be seen more clearly in Figs 4 and 5, where the effect of the heating rate on the dull (wheel) surface diffraction pattern is shown. Since RED results are often ambiguous without information on the surface morphology, SEM micrographs were taken from the dull side of Metglas 2605-SC before and after heat treatment, and are shown in Figs 5c and f. Both of these micrographs show very smooth surfaces, and the observed orientation in the diffraction pattern is not thought to be a morphology-related artefact. The corresponding time–temperature curves for these sequences are again summarized in Fig. 6, and it is

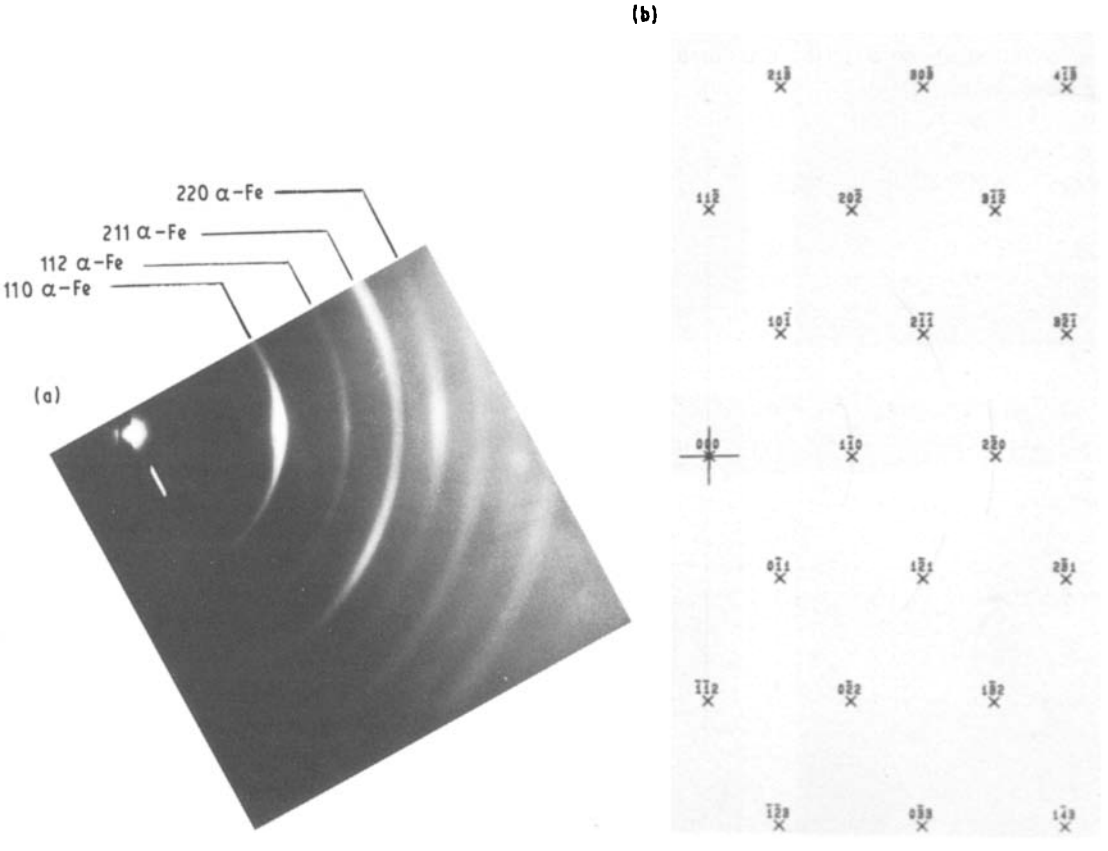

Figure 3 (a, b) Indexed diffraction pattern of ferrite taken on crystallized Metglas 2605-SC. Camera constant = 0.627 nm. [1 1 1] surface orientation, bcc α-Fe.

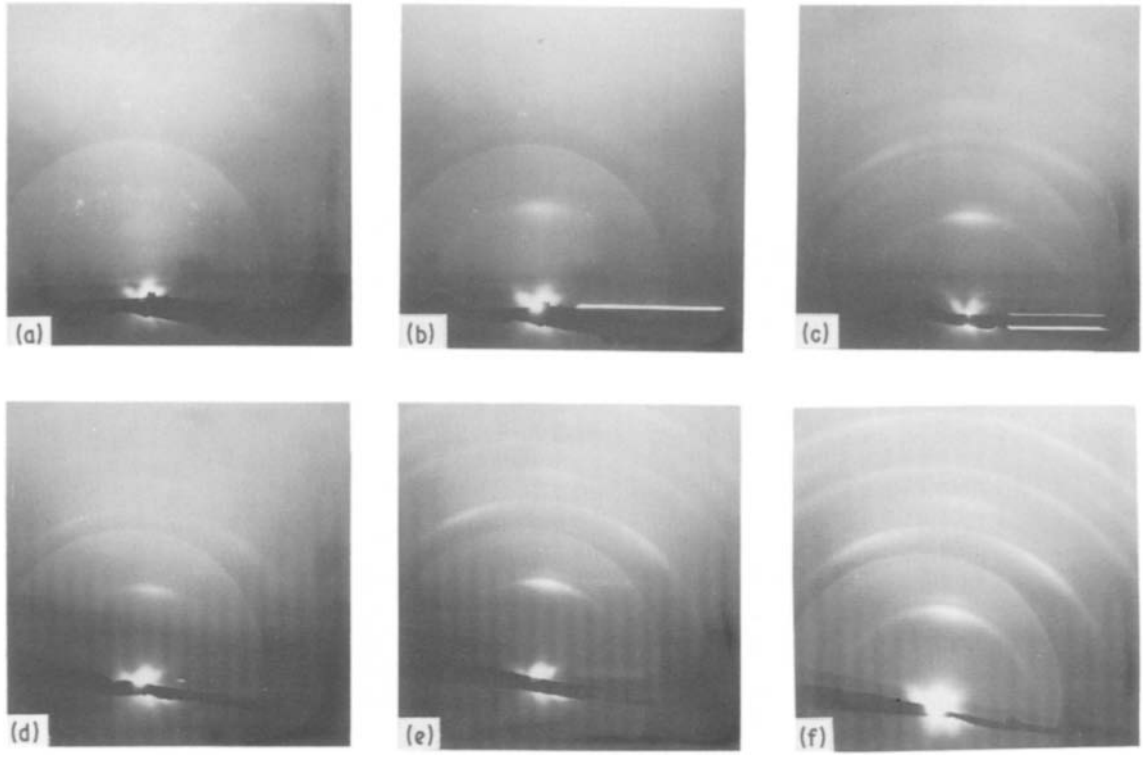

Figure 4 (a–c) RED sequence taken during crystallization of the dull side of Metglas 2605-SC with a heater current of 0.85 A; (d–f) RED sequence taken with a heater current of 1.7 A.

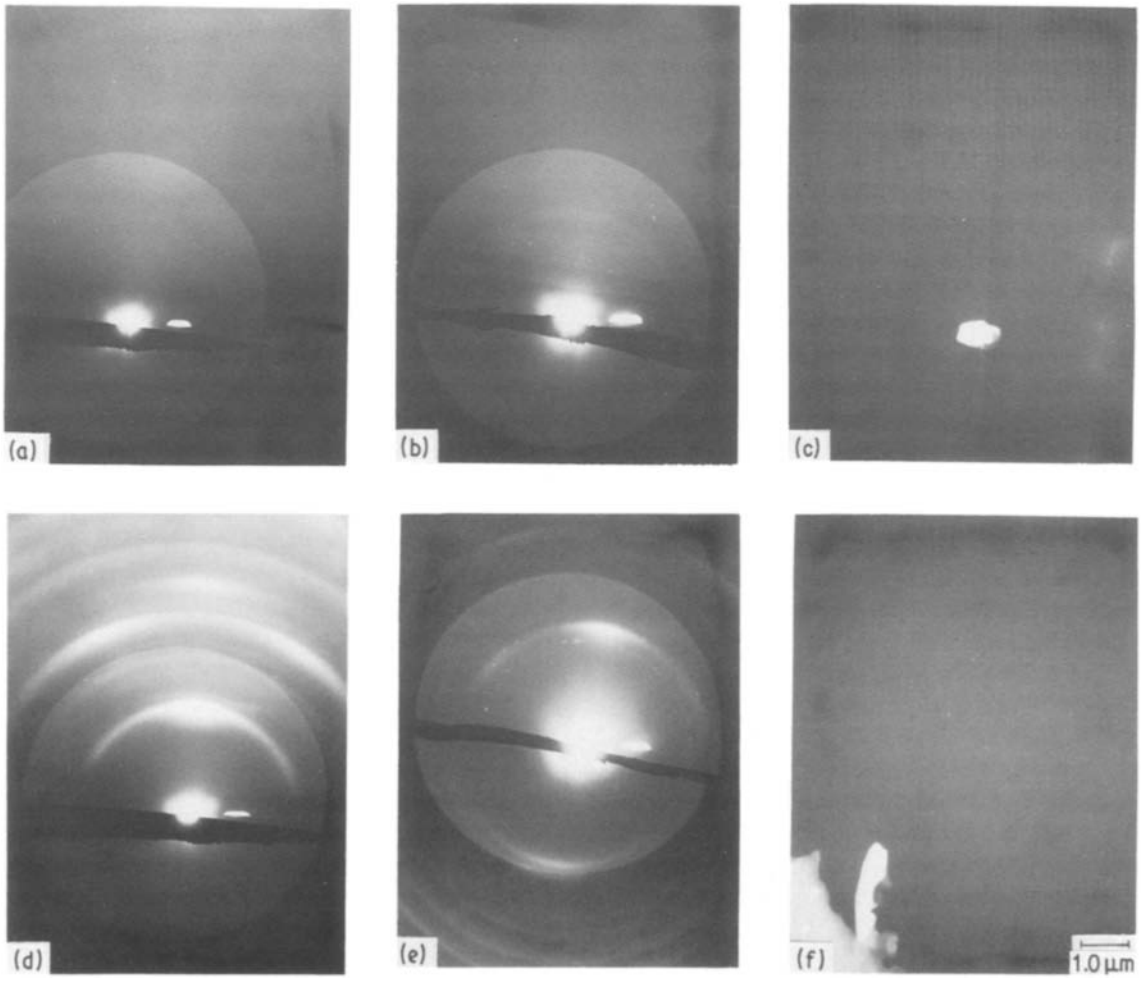

Figure 5 (a, d) RED patterns of dull side of 2605-SC before and after heating with a current of 1.5 A; (b, e) RED patterns of dull side of 2605-SC before and after heating with a current of 1.0 A; (c, f,) SEM micrographs of dull side of 2605-SC before and after exposure to 673 K.

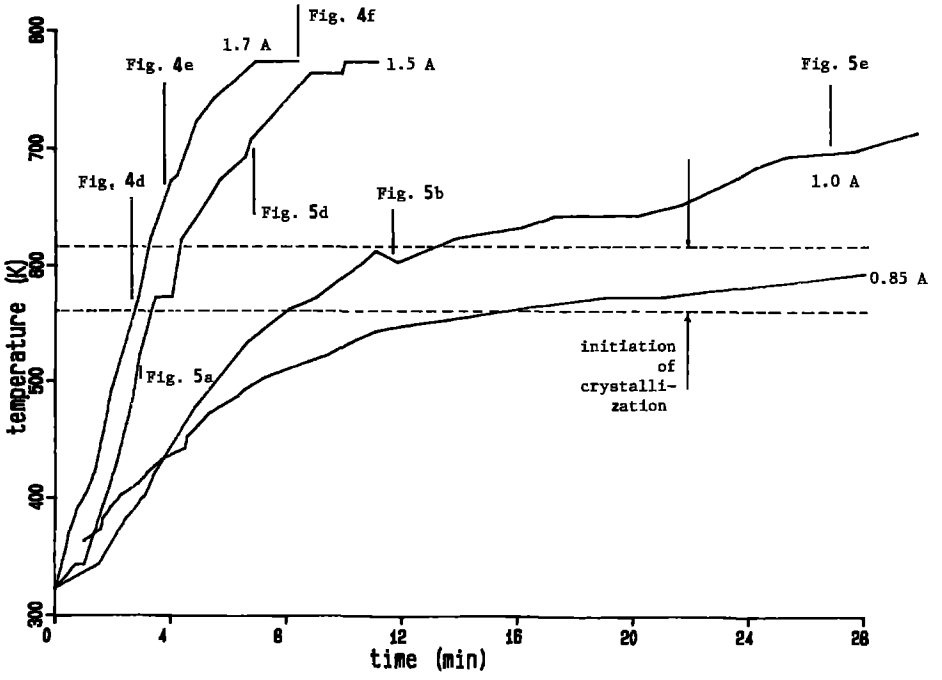

Figure 6 Time–temperature curves for the dull side of Metglas 2605-SC during *in situ* heat treatment.

seen that the surface orientation is evident throughout a wide range of heating rates.

In Figs 2 and 6, where the heater currents are shown, the heat-treatment conditions are seen to be very reproducible. If the initiation of crystallization during the heat treatments is noted as the time at which the first ring pattern is visible, a difference between that initiation temperature on the dull and shiny side is evident. The dull side, which is the fastest cooled side, is found to crystallize approximately 40° C below the shiny side of the ribbon. This observation suggests that crystallinity initiates earlier on the side closest to the wheel, presumably as a result of a higher driving force towards crystallinity or a larger short-range diffusivity associated with a more open structure.

3.1.2. Effect of coating on substrate crystallization

When the topmost layer is removed with 600 grit SiC grinding paper, the diffraction pattern after crystallization corresponds to unoriented ferrite crystallites

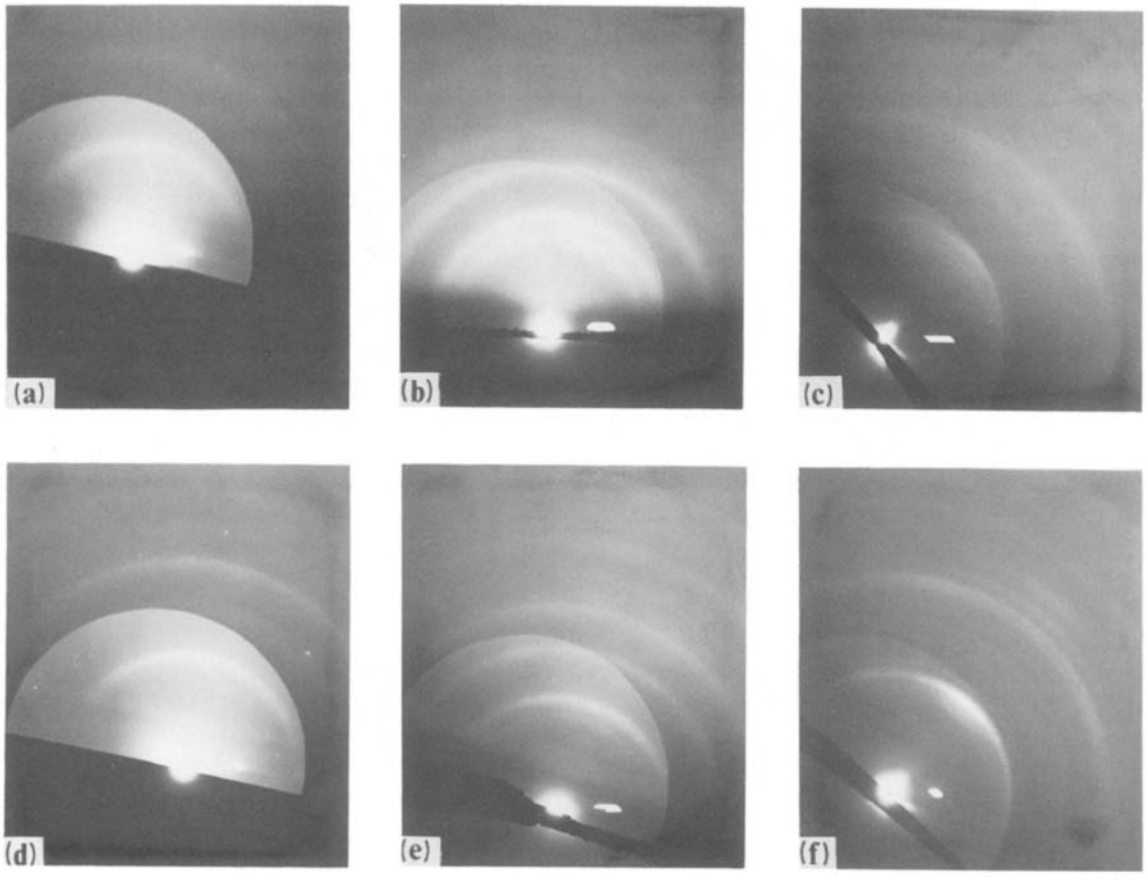

Figure 7 (a, d) RED pattern of dull side of 2605-SC ground with 600 grit SiC; (b, e) RED pattern of dull side of 2605-SC oxidized in water; (c, f) RED pattern of dull side of 2605-SC with Au–Pd sputter deposit.

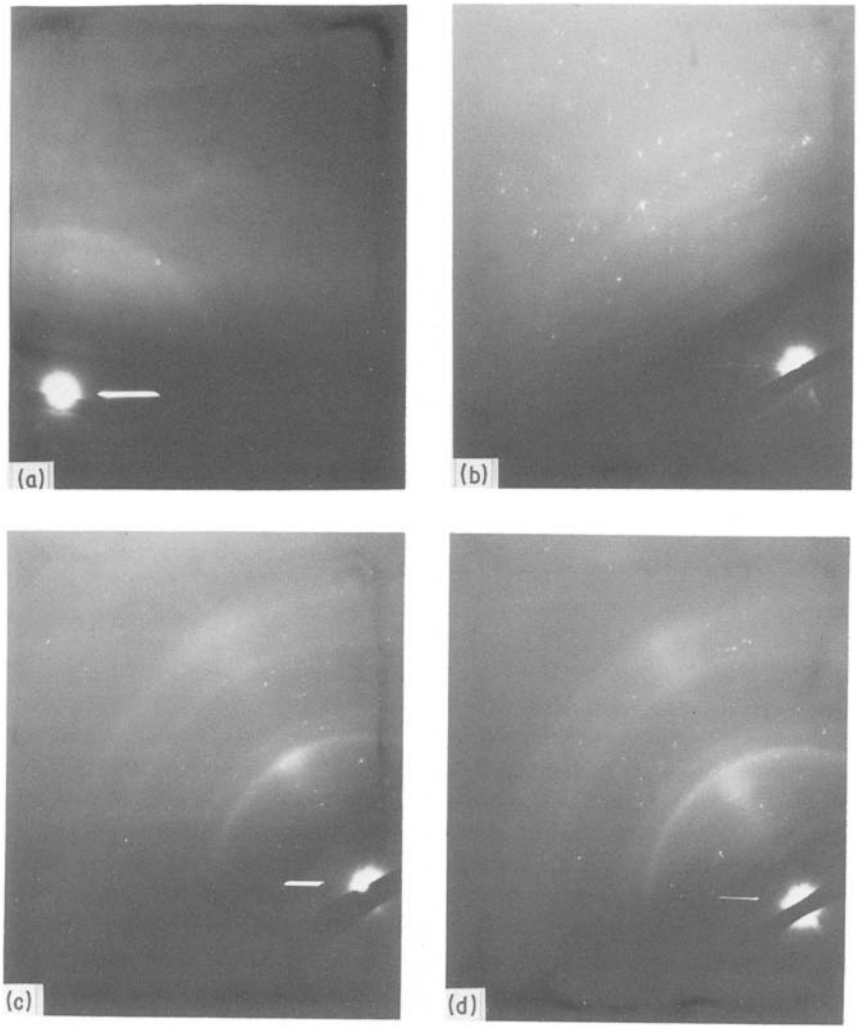

Figure 8 (a–d) RED sequence of dull side of Metglas 2826-MB.

(Figs 7a and d). It is therefore evident that the orientation in the ferrite crystallites is a localized surface phenomenon and is explainable by surface contamination or by local elemental depletion or enrichment of the surface. In order to investigate this effect, the dull side of the ribbon was artificially oxidized in water and observed during crystallization. If, on the other hand, the surface is covered by a thin Au–Pd film, sputter-deposited in a nitrogen plasma, the RED pattern of the underlying crystallized substrate reveals an arc pattern of ferrite, and crystallite orientation is again present (Figs 7c and f). The orientation of the immediate surface observed in Metglas 2605-SC is therefore thought to be a result of local enrichment or depletion of the surface, which can be suppressed by oxidation of the surface layer, and is not a result of heterogeneous nucleation of crystallites from the free surface.

3.2. Metglas 2826-MB

3.2.1. Heat treatments

During heat treatment of 2826-MB, the sequence of crystallization is observed to support previous X-ray diffraction studies [2]. A typical crystallization experiment at relatively low temperature (< 773 K) is shown in Figs 8a to d, taken off the wheel side of the metglas ribbon. The emergence of Fe–Ni diffraction rings, which in this case do not crystallize according to any orientation, can be followed. If the bright (free) side of the ribbon is heated to high temperatures (> 773 K), a Fe–Ni–B pattern is observed to emerge. If, however, the bright side of the ribbon is observed during low temperatures (573 to 743 K, Figs 9d to f) heat treatments, an oriented fcc arc pattern, which can be indexed to Fe–Ni, is detected at the surface. The surface orientation corresponds in this case to the [1 1 0] direction, as can be seen from Fig. 10. At high temperatures, the X-ray diffraction results closely match the RED observation, and both diffraction patterns correspond to cubic Fe–Ni boride. However, X-ray diffraction results taken from the ribbons exposed to lower temperatures predict a predominance of Fe–Ni boride, whereas the surface RED patterns of the same samples show very clear diffraction rings of fcc Fe–Ni. This discrepancy, as well as the orientation in the diffraction patterns, is again explainable by surface contamination or by the chemical depletion of the immediate surface layer.

3.2.2. Effect of coating on substrate crystallization

If the bright side of the Metglas 2826-MB ribbon is observed during heat treatment at low temperatures, some surface upheaval is observed, and the RED pattern shows a weak orientation of the Fe–Ni rings. A thin (1.2 nm) platinum layer affects the crystallization sequence of the underlying substrate, resulting in an apparently unoriented ring pattern of Fe–Ni

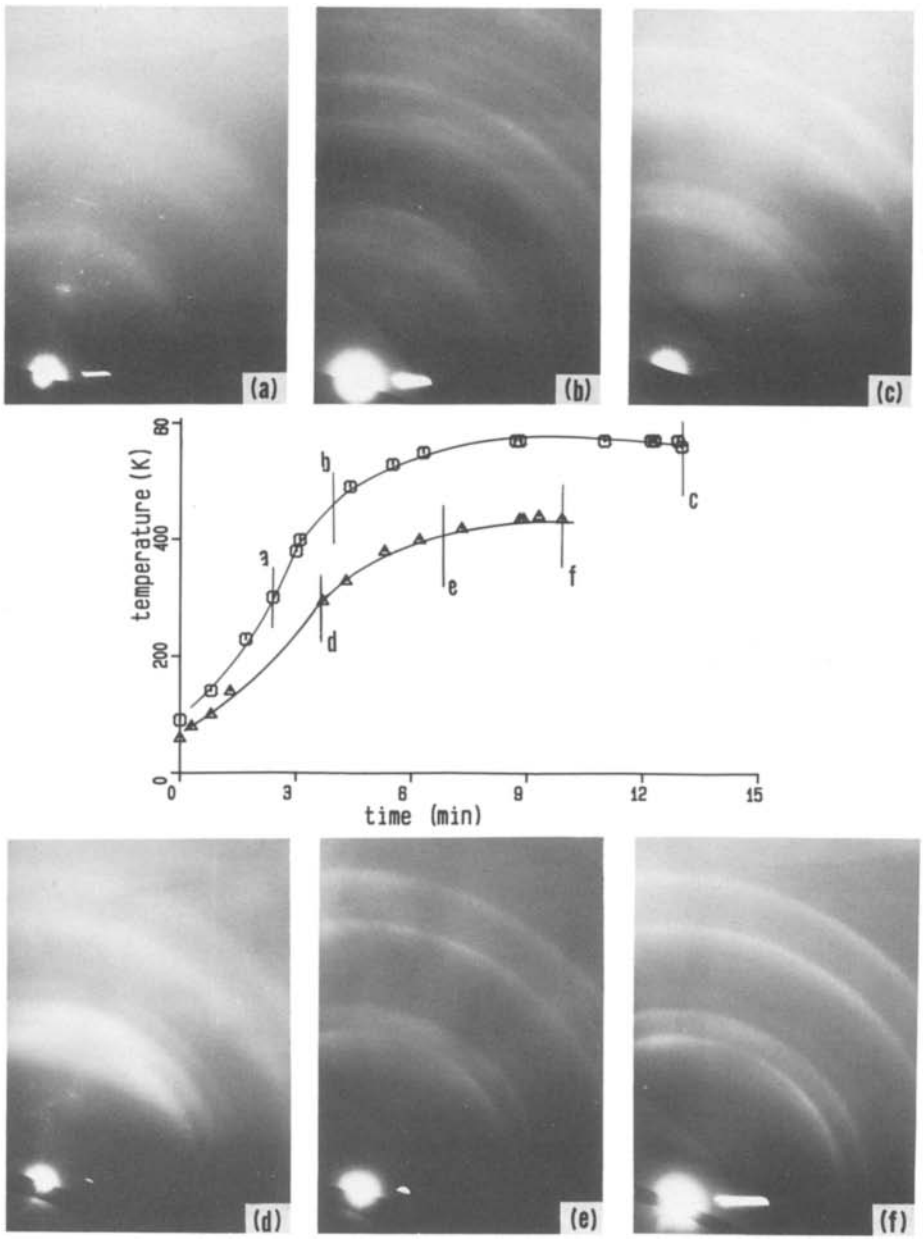

Figure 9 (a–c) RED sequence of bright side of 2826-MB heated with high heating rate; (d–f) RED sequence of 2826-MB heated with low heating rate.

(Fig. 11b), which is superimposed on the original platinum pattern (Fig. 11a). This lack of an orientation is not necessarily indicative of an influence of the platinum coating on the crystallization behaviour of the substrate, but can instead be explained by dissolution of the surface layer during platinum deposition in the chloroplatinic acid plating bath. Experiments with sputter-coated Au–Pd films enforce this contention, and a weak orientation of the substrate crystallites is evident when such overlayers are used in crystallization experiments.

4. Summary and conclusions

A definite difference between the crystallization behaviour of the bulk and surface of amorphous Metglas 2826-MB and 2065-SC ribbons can be seen during *in situ* heat treatment observations by RED. If the dull (wheel) surface of 2605-SC is observed without further preparation, the diffraction pattern is an arc pattern with a [1 1 1] surface orientation. The RED pattern sequences obtained in this metglas were not influenced by heating rates or exposure temperatures within the temperature ranges investigated. When, however, this surface is ground with 600 grit SiC paper, or if the bright side of the metglas ribbon is observed, this orientation is no longer noticeable. The surface orientation can also be suppressed by oxidizing the surface, but is unaffected by a thin sputter-coated Au–Pd overlayer.

In 2826-MB, on the other hand, a difference between the RED and X-ray diffractometer patterns is evident, indicating different crystallization species at the surface and in the bulk. An Fe–Ni RED pattern is predominant after exposure to low temperatures, whereas at higher temperatures the surface consists mainly of Fe–Ni boride. An Fe–Ni arc pattern indicating crystallite orientation can be observed on the bright (free) side of the metglas ribbon, which is apparently suppressed after electrodeposition of a platinum layer on the surface. However, this is thought to be a result of the dissolution of the surface layer during such plating.

Preferred orientation of the crystallites of amorphous metglas ribbons is therefore a localized surface

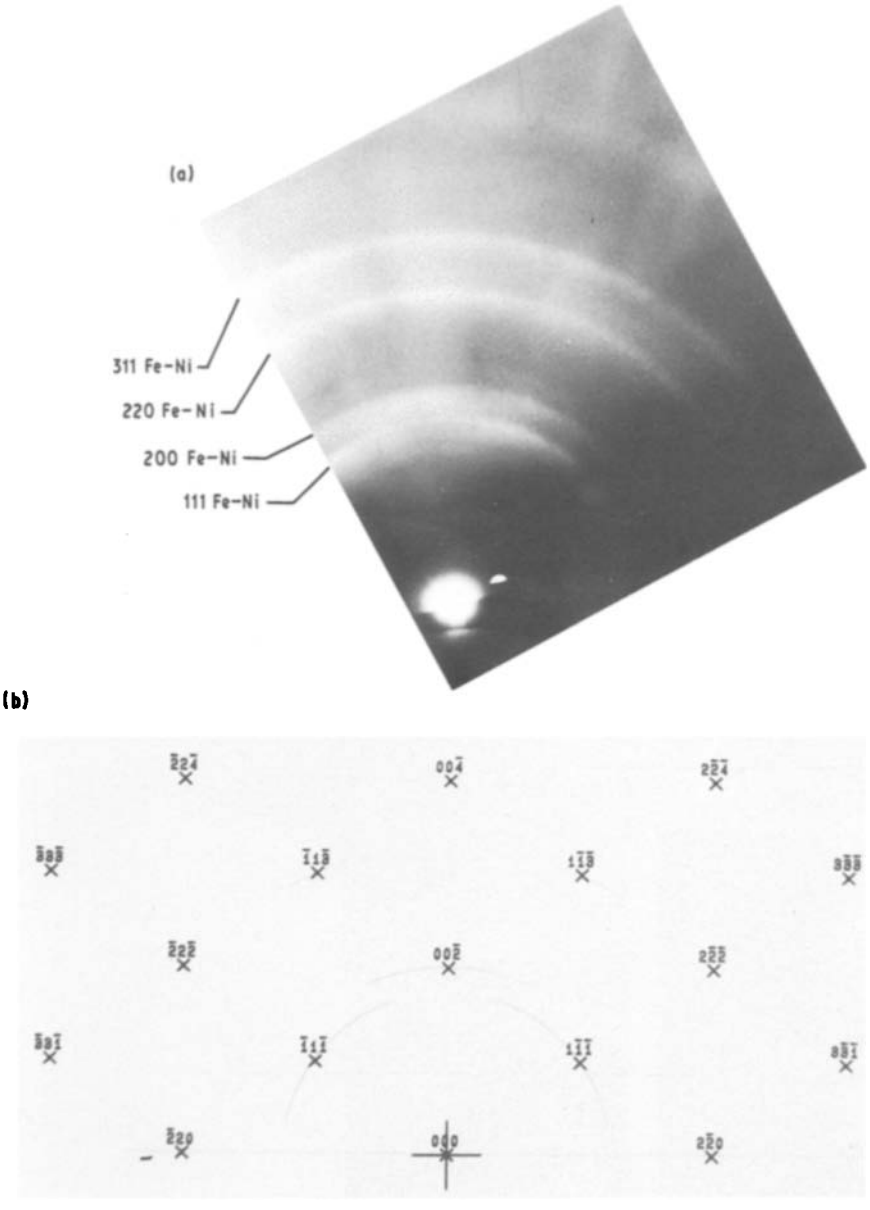

Figure 10 (a, b) Indexed RED pattern of bright side of 2825-MB heat treated to 673 K. Camera constant = 0.627 nm. [1 1 0] surface orientation, fcc Fe–Ni.

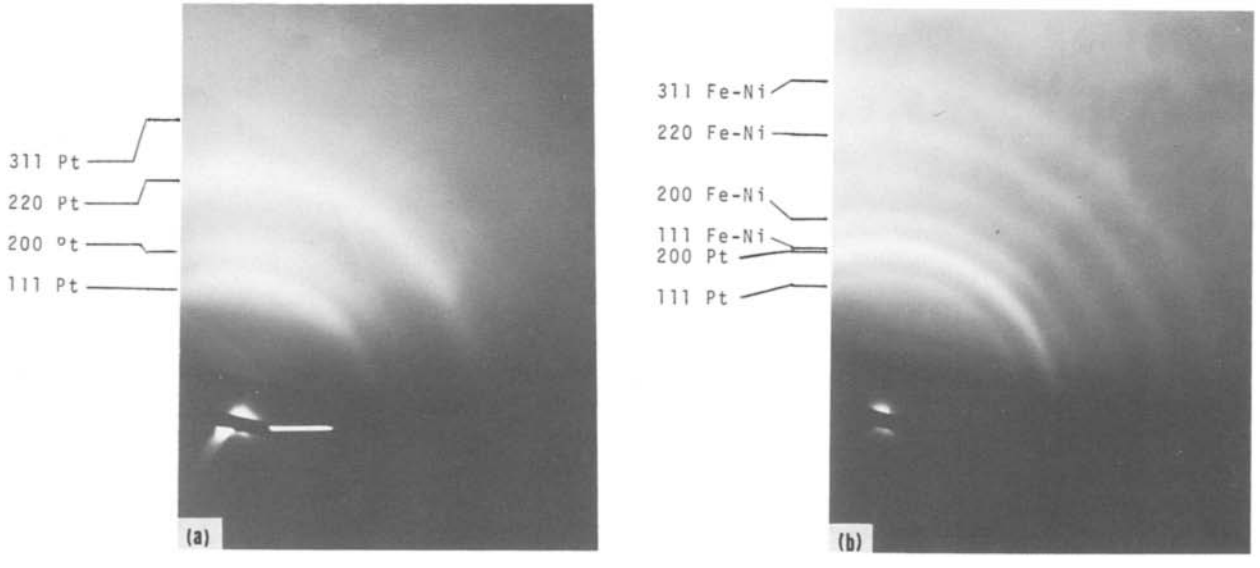

Figure 11 (a, b) Heat-treated sequence of platinum-plated (1.2 nm) Metglas 2826-MB.

phenomenon. Since the surface layer of metglas ribbons is easily removed during grinding, oxidation, or chemical etching, preferred orientation of crystallites is not observed in TEM and FIM observations. Since the sampling depth of RED generally ranges only up to some tens of nanometres [15], this technique allows the investigation of the cause of this anomalous phenomenon. The anisotropic crystallization behaviour could be suppressed by intentional oxidation of the surface, and therefore this phenomenon is thought to be a result of elemental depletion of the surface instead of surface contamination. This conclusion coincides with previous CEMS work [3], which showed local depletion of silicon as well as enrichment of carbon and boron on Metglas 2605-SC surfaces.

Acknowledgement

This study was funded by a Department of Energy, Division of Materials Science contract DE-ER-78-04-4266, which is gratefully acknowledged.

References

1. U. KOESTER and U. HEROLD, "Crystallization of Metallic Glasses" in *Topics in Applied Physics*, Vol. 46, edited by H. J. Guentherodt and H. Beck (Springer Verlag, 1981) p. 239.
2. O. T. INAL, A. SCHERER, E. G. REINEKE and M. J. BORDEN, *Thin Solid Films* **119** (1984) 395.
3. N. SAEGUSA and A. H. MORRISH, *Phys. Rev.* **B26** (1982) 6547.
4. J. L. WALTER, S. F. BARTAM and R. R. RUSSELL, *Met. Trans.* **9A** (1978) 803.
5. K. P. MIZGALSKI, O. T. INAL, F. G. YOST and M. M. KARNOWSKY, *J. Mater. Sci.* **16** (1981) 3357.
6. J. PILLER and P. HAASEN, *Acta Metall.* **30** (1982) 1.
7. C. ANTONIONE, L. BATTEZZATI, A. LUCCI, G. RIONTINO and G. VENTURELLO, *Scripta Metall.* **12** (1978) 1011.
8. K. OSAMURA, K. SHIBUE, R. SUZUKI, Y. MURAKAMI and S. TAKAYAMA, *J. Mater. Sci* **16** (1981) 957.
9. H. G. SUZUKI and K. YAMAMOTO, *Mater. Sci. Eng.* **33** (1978) 57.
10. J. L. WALKER, F. BACON and F. E. LUBORSKY, *ibid.* **24** (1976) 239.
11. N. SAEGUSA and A. H. MORRISH, *Phys. Rev.* **B26** (1982) 305.
12. A. SHERER and O. T. INAL, *Thin Solid Films* **119** (1984) 415.
13. J. C. SWARTZ, J. J. HAUGH, R. F. KRAUSE and R. KOSSOWSKY, *J. Appl. Phys.* **52** (1981) 1908.
14. P. G. BOSWELL, *J. Mater. Sci.* **15** (1980) 1926.
15. H. RAETHER, *Ergeb. Exakten Naturwiss.* **24** (54) (1951) 127.

Received 22 August 1985
and accepted 6 May 1986